

COVER PAGE

Document downloaded by @DAEL

Sat Nov 28 09:04:13 2026
For personal use

When automatic English translation is provided, only the original document is authentic.
The EAA cannot be held responsible of any translation error

Bibliographical reference

Singularities in First-Order Wedge-Diffraction Expressions within Narrow, Finite 3D Wedges, Paul T. Calamia and U. Peter Svensson, Acta Acustica **vol. 97** (Number 3), 2011, pp. 525-529

DOI
https://doi.org/10.3813/AAA.918433

ACTA ACUSTICA UNITED WITH ACUSTICA
Vol. 97 (2011) 525 – 529

DOI 10.3813/AAA.918433

Singularities in First-Order Wedge-Diffraction Expressions within Narrow, Finite 3D Wedges

Paul T. Calamia[1], U. Peter Svensson[2]
[1] Cambridge, MA, USA. pcalamia@cs.princeton.edu
[2] Acoustics Research Centre, Department of Electronics and Telecommunications, Norwegian University of Science and Technology, 7491 Trondheim, Norway

PACS no. 43.20.El

Abstract

The field resulting from propagating sound interacting with a wedge is often decomposed into geometrical-acoustics (GA) and diffracted components. With such a decomposition, singularities in mathematical expressions for the latter typically are explained as necessary to compensate for discontinuities in the GA field at the two shadow boundaries and the two first-order reflection boundaries corresponding to the two wedge faces. However, these singularities result from periodic functions and thus can be associated with additional, higher-order GA components. In this short communication we describe the relationship between the periodicity of the diffraction singularities and higher-order reflections, which is relevant to the analysis of wedges with open angle less than π. The discussion is provided specifically in the context of finite, three-dimensional wedges.

1. Introduction

The sound field resulting from propagation in the vicinity of a wedge is often analyzed in terms of its constituent parts: the geometrical-acoustics (GA) components, *i.e.* the direct sound and specular reflections, and the diffraction from the edge formed by the intersection of the two wedge faces. With such a decomposition, singularities in mathematical formulae for the diffracted component typically are explained as necessary to compensate for the discontinuities in the GA field at the two shadow boundaries and at the two first-order reflection boundaries. However, these singularities result from periodic functions, and thus can be associated with additional, higher-order GA components. Understanding this behavior is critical for numerical implementations of diffraction expressions, such as the one described in [1], where integration across a singularity can lead to significant errors in the onset amplitude of a diffraction impulse response.

In this short communication, we describe the relationship between the periodicity of the singularities in first-order diffraction expressions and higher-order reflections, which is specifically relevant to the evaluation of soundfields in the presence of a wedge with an open angle less than π, *i.e.* wedges which support multiple reflections between their faces. While "narrow" wedges have been studied previously (*e.g.* in [2, 3]), and the multiple-reflection behavior within them is well understood (*e.g.* see [4, 5]) the analyses have been provided almost exclusively in the context of infinite wedges and plane-wave incidence (*e.g.* using the Malyuzhinets theory as described in [6]). Here, the time-domain Biot-Tolstoy-Medwin (BTM) diffraction formulation presented by Svensson *et al.* [7] is utilized for the analysis of a *finite-length* wedge insonfied by a point source at an arbitrary distance, but the results are equally applicable to the frequency-domain BTM formulation [8] as well as to other diffraction expressions.

Received 16 August 2010,
accepted 18 January 2011.

2. The BTM Diffraction Formulation

Consider an edge formed by the intersection of two rigid, planar facets, a point source S, and a receiver R. Using an edge-aligned cylindrical-coordinate system (with the z-axis along the edge), the source and receiver positions are given by (r_S, θ_S, z_S) and (r_R, θ_R, z_R), respectively, and the continuous-time diffraction impulse response (IR) is given as an integral along the edge [7],

$$h(\tau) = -\frac{\nu}{4\pi} \sum_{i=1}^{4} \int_{z_1}^{z_2} \delta\left(\tau - \frac{m+l}{c}\right) \frac{\beta_i}{ml}\, \mathrm{d}z, \tag{1}$$

where $\nu = \pi/\theta_W$ is the wedge index, θ_W is the open wedge angle, δ is the Dirac delta function, m and l are the distances from S and R, respectively, to a position, z, on the edge, and c is the speed of sound. If the edge is of finite length, the z-coordinate values of the edge endpoints are used for the integration limits. Otherwise $z_1 = -\infty$ and $z_2 = \infty$. The functions β_i are

$$\beta_i = \frac{\sin(\nu\varphi_i)}{\cosh(\nu\eta) - \cos(\nu\varphi_i)}, \tag{2}$$

where the angles φ_i are

$$\begin{aligned} \varphi_1 &= \pi + \theta_S + \theta_R, \qquad \varphi_2 = \pi + \theta_S - \theta_R, \\ \varphi_3 &= \pi - \theta_S + \theta_R, \qquad \varphi_4 = \pi - \theta_S - \theta_R, \end{aligned} \tag{3}$$

and the auxiliary function η is

$$\eta = \cosh^{-1}\left\{\frac{ml + (z - z_S)(z - z_R)}{r_S r_R}\right\}. \tag{4}$$

Equation (2), and thus the integrand in equation (1), is subject to a singularity when $\cosh(\nu\eta) = \cos(\nu\varphi_i) = 1$. $\cosh(\nu\eta) = 1$ for the shortest path from the source, via the edge, to the receiver, and thus the singularity occurs at the onset of the diffraction IR. $\cos(\nu\varphi_i) = 1$ for receiver positions at the reflection and shadow boundaries (depicted in Figure 1), *i.e.* the locations where the geometrical-acoustics components (the direct sound and specular reflection) experience discontinuities. It is the cosine term which is of particular interest here.

3. Singularities

For the following analysis, we assume that the cylindrical-coordinate system is aligned with one face, F_1, located at $\theta = 0$ and the other, F_2, at $\theta = \theta_W$. Values of $\nu\varphi_i$ that cause a singularity in the β_i functions at the onset of the diffraction IR, *i.e.* values for which $\cos(\nu\varphi_i) = 1$, are considered.

© S. Hirzel Verlag · EAA

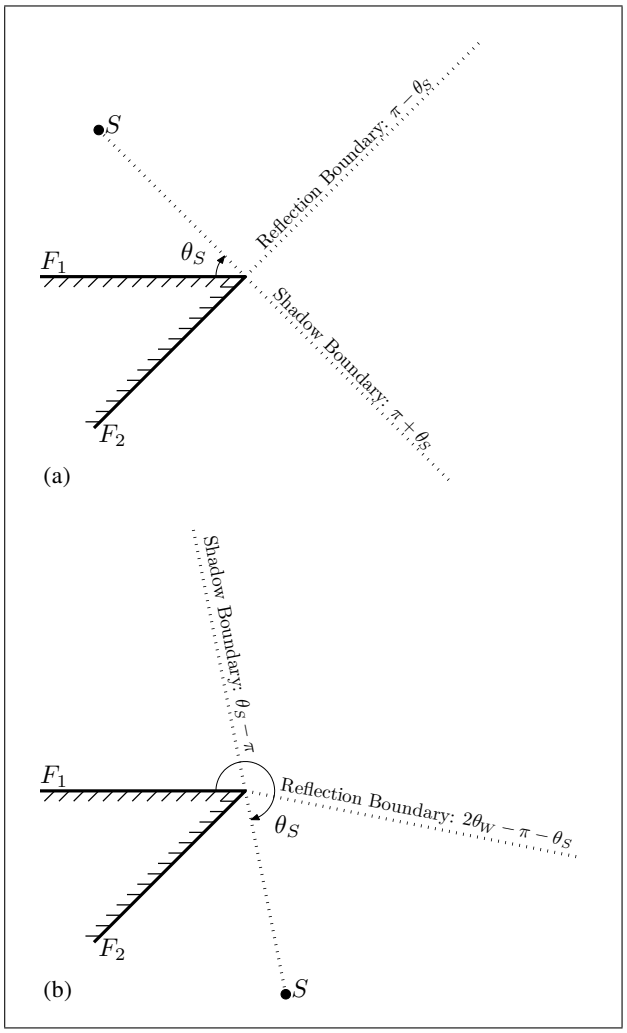

Figure 1. Example geometry for the four basic singularity cases. (a) $\theta_S < \pi$: $\nu\varphi_2 = 0$ at the shadow boundary and $\nu\varphi_4 = 0$ at the reflection boundary. (b) $\theta_S > \pi$: $\nu\varphi_3 = 0$ at the shadow boundary and $\nu\varphi_1 = 2\pi$ at the reflection boundary.

3.1. Singularities related to the direct sound and first-order specular reflections

The four terms of equation (1) typically are associated with the two shadow boundaries and two first-order reflection boundaries dictated by the wedge faces and shown in Figure 1. For a source with visibility to F_1 ($\theta_S < \pi$), the shadow boundary is located at $\theta_{SB} = \pi + \theta_S$. For a receiver located on this boundary (*i.e.* $\theta_R = \pi + \theta_S$),

$$\nu\varphi_2 = \nu\left[\pi + \theta_S - (\pi + \theta_S)\right] = 0. \tag{5}$$

The reflection boundary is located at $\theta_{RB} = \pi - \theta_S$, and for a receiver located on this boundary,

$$\nu\varphi_4 = \nu\left[\pi - \theta_S - (\pi - \theta_S)\right] = 0. \tag{6}$$

For a source with visibility to F_2 ($\theta_S > \pi$), the shadow boundary is located at $\theta_{SB} = \theta_S - \pi$. For a receiver located on this boundary,

$$\nu\varphi_3 = \nu\left[\pi - \theta_S + (\theta_S - \pi)\right] = 0. \tag{7}$$

The reflection boundary is located at $\theta_{RB} = 2\theta_W - \pi - \theta_S$, and for a receiver located on this boundary,

$$\begin{aligned} \nu\varphi_1 = \nu\left[\pi + \theta_S + (2\theta_W - \pi - \theta_S)\right] &= \frac{\pi}{\theta_W} \cdot 2\theta_W \\ &= 2\pi. \end{aligned} \tag{8}$$

An alternative method to identify the values of $\nu\varphi_i$ associated with singularities at reflection boundaries involves finding the angular coordinate of the image source that gives rise to the reflection, then evaluating the appropriate *shadow-boundary* condition for that image source. For example, the image source for a reflection from F_1 is located at $\theta'_S = -\theta_S$. Replacing θ_S with θ'_S in equation (5), the shadow-boundary condition for F_1, yields

$$\begin{aligned} \nu\varphi'_2 &= \nu\left[\pi + \theta'_S - \theta_R\right] \\ &= \nu\left[\pi - \theta_S - \theta_R\right] = \nu\varphi_4 = 0, \end{aligned} \tag{9}$$

a result equivalent to equation (6). Similarly, mirroring S about θ_W yields $\theta'_S = 2\theta_W - \theta_S$ for the image source associated with the first-order reflection from F_2. Replacing θ_S with θ'_S in equation (7) yields

$$\begin{aligned} \nu\varphi'_3 = \nu[\pi - \theta'_S + \theta_R] &= 0, \\ \nu[\pi - 2\theta_W + \theta_S + \theta_R] &= 0, \\ \pi + \theta_S + \theta_R &= 2\theta_W, \\ \varphi_1 &= 2\theta_W, \\ \nu\varphi_1 &= 2\pi, \end{aligned} \tag{10}$$

which is equivalent to equation (8).

3.2. Singularities related to higher-order specular reflections

For a wedge with $\theta_W < \pi$, higher-order specular reflections can occur between the faces. To understand the first-order diffraction from such a wedge completely, all possible singularities caused by $\cos(\nu\varphi) = 1$, *i.e.* all possible conditions for which $\nu\varphi_i = 2n\pi$ for integer values of n, must be considered. Using the image-source approach described above, higher-order reflection boundaries can be associated with the appropriate singularity-causing values of $\nu\varphi_i$. For example, consider the reflection path $S \to F_2 \to F_1 \to R$. The corresponding image source is located at $\theta''_S = \theta_S - 2\theta_W$. Substituting this into equation (5) yields

$$\begin{aligned} \nu\varphi''_2 = \nu[\pi + \theta''_S - \theta_R] &= 0, \\ \nu[\pi + \theta_S - 2\theta_W - \theta_R] &= 0, \\ \pi + \theta_S - \theta_R &= 2\theta_W, \\ \varphi_2 &= 2\theta_W, \\ \nu\varphi_2 &= 2\pi. \end{aligned} \tag{11}$$

Similarly, the boundary for the reflection $S \to F_1 \to F_2 \to R$ corresponds to $\nu\varphi_3 = 2\pi$, and that for $S \to F_1 \to F_2 \to F_1 \to R$ corresponds to $\nu\varphi_4 = 2\pi$. Further values of $2n\pi$ and the associated reflection boundaries are given in Table I, and the table can be generalized as follows for $n > 0$. Given a singularity due to $\nu\varphi_i = 2n\pi$, the final surface in the associated reflection path is F_j where

$$j = \begin{cases} 1 & \text{if } 2n + i \text{ is even} \\ 2 & \text{if } 2n + i \text{ is odd,} \end{cases} \tag{12}$$

and the number of surfaces in the reflection path, s, is

$$s = 2n + \frac{i - j - 1}{2}. \tag{13}$$

To bound n, recall that with the wedge faces at $\theta = 0$ and θ_W, the minimum value of θ_S and of θ_R is 0 and the maximum value for

Table I. Geometrical-acoustics components associated with the four $\nu\varphi_i$ angles at $2n\pi$ for $n = 0, 1, 2, 3$. S is the source, R is the receiver, and $F_{1,2}$ are the two wedge faces.

	0	2π	4π	6π
$\nu\varphi_1$	N/A	$S \to F_2 \to R$	$S \to F_2 \to F_1 \to F_2 \to R$	$S \to F_2 \to F_1 \to F_2 \to F_1 \to F_2 \to R$
$\nu\varphi_2$	$S \to R$ (S sees F_1)	$S \to F_2 \to F_1 \to R$	$S \to F_2 \to F_1 \to F_2 \to F_1 \to R$	$S \to F_2 \to F_1 \to F_2 \to F_1 \to F_2 \to F_1 \to R$
$\nu\varphi_3$	$S \to R$ (S sees F_2)	$S \to F_1 \to F_2 \to R$	$S \to F_1 \to F_2 \to F_1 \to F_2 \to R$	$S \to F_1 \to F_2 \to F_1 \to F_2 \to F_1 \to F_2 \to R$
$\nu\varphi_4$	$S \to F_1 \to R$	$S \to F_1 \to F_2 \to F_1 \to R$	$S \to F_1 \to F_2 \to F_1 \to F_2 \to F_1 \to R$	$S \to F_1 \to F_2 \to F_1 \to F_2 \to F_1 \to F_2 \to F_1 \to R$

both is θ_W. This implies that the minimum and maximum values of φ_i are

$$\begin{aligned} \varphi_{min} &= \varphi_4\Big|_{(\theta_S=\theta_W,\theta_R=\theta_W)} = \pi - 2\theta_W, \\ \varphi_{max} &= \varphi_1\Big|_{(\theta_S=\theta_W,\theta_R=\theta_W)} = \pi + 2\theta_W, \end{aligned} \tag{14}$$

and the corresponding minimum and maximum values of $\nu\varphi_i$ are

$$\begin{aligned} \nu\varphi_{min} &= \nu(\pi - 2\theta_W) = \nu\pi - 2\pi = (\nu - 2)\pi, \\ \nu\varphi_{max} &= \nu(\pi + 2\theta_W) = \nu\pi + 2\pi = (\nu + 2)\pi. \end{aligned} \tag{15}$$

The minimum value of ν is $1/2$ (when $\theta_W = 2\pi$), therefore $\nu\varphi_{min} \geq -3\pi/2$ and the singularity due to $\nu\varphi_i = -2\pi$ (or $\nu\varphi_i = 2n\pi$, $n \leq -1$) will never occur. Thus, in general, values of $\nu\varphi_i$ for which a singularity *can* occur take the form

$$\nu\varphi_i = 2n\pi, n = 0, 1, ..., \left\lfloor \frac{\nu+2}{2} \right\rfloor. \tag{16}$$

For a specific wedge, the lower bound for n is $\left\lceil \frac{\nu-2}{2} \right\rceil$. Note that $\nu\varphi_i = 0$ only occurs for $i = 2, 3, 4$ because $\nu > 0$ and $\varphi_1 = \pi + \theta_S + \theta_R > 0$.

3.3. Maximum two singularities

As illustrated in the previous section and in Table I, there are many possibilities for singularities related to higher-order reflections in narrow wedges. Interestingly, however, there can never be more than two singularities for a specific combination of wedge angle and source position. This can be understood by looking at the relationship which must be fulfilled for a singularity, given by equation (16), which can be solved for the receiver angle θ_R that experiences a singularity. Each of the four equations which has a solution within $[0, \theta_W]$ indicates a receiver position which has a singularity,

$$\theta_R = -\pi + n_1 \cdot 2\theta_W - \theta_S, \tag{17}$$
$$\theta_R = \pi - n_2 \cdot 2\theta_W + \theta_S, \tag{18}$$
$$\theta_R = -\pi + n_3 \cdot 2\theta_W + \theta_S, \tag{19}$$
$$\theta_R = \pi - n_4 \cdot 2\theta_W - \theta_S, \tag{20}$$

where n_i can be any non-negative integers and $\theta_S \in [0, \theta_W]$. The question is whether or not more than two of the equations (17-20) can have a solution. The discussion which immediately follows assumes that $\theta_R \in]0, \theta_W[$, and in a separate study below it will be shown that the cases where singularity-causing receiver positions are on one of the two wedge faces vanish.

Because of the similarity of equations (17) and (18), a first test should determine whether both can have valid solutions. The requirement that $\theta_R \in]0, \theta_W[$ for equation (17) leads to

$$\begin{aligned} \frac{\pi + \theta_S}{2\theta_W} < n_1 < \frac{\pi + \theta_S}{2\theta_W} + 0.5, \\ \to c_1 < n_1 < c_1 + 0.5, \end{aligned} \tag{21}$$

where c_1 is a real-valued constant. For an integer n_1 to satisfy this, the decimal part of c_1 must be larger than 0.5. Using the same constant c_1, the requirement that $\theta_R \in]0, \theta_W[$ for equation (18) leads to

$$\to c_1 - 0.5 < n_2 < c_1, \tag{22}$$

which implies a contradictory requirement that the decimal part of c_1 be smaller than 0.5. Therefore, equations (17) and (18) cannot be true for the same combination of θ_W and θ_S.

A second similar test can determine whether or not equations (19) and (20) both can have solutions. Equation (19) leads to

$$\begin{aligned} \frac{\pi - \theta_S}{2\theta_W} < n_3 < \frac{\pi - \theta_S}{2\theta_W} + 0.5, \\ \to c_2 < n_3 < c_2 + 0.5, \end{aligned} \tag{23}$$

where c_2 is a real-valued constant. Equation (23) implies that the decimal part of c_2 must be larger than 0.5. Equation (20) leads to the requirement that

$$\to c_2 - 0.5 < n_4 < c_2. \tag{24}$$

This implies that the decimal part of c_2 must be smaller than 0.5, which is contradictory to the requirement in equation (23) so equations (19) and (20) can never both have a solution. These two tests remove any possibility to get solutions to three or four of equations (17-20). Therefore there can be maximum two singularities for any combination of wedge and source position.

As mentioned above, some special cases have not yet been considered, namely those where singularity-causing receiver positions are on one of the wedge faces, *i.e.*, $\theta_R = 0$ or $\theta_R = \theta_W$. In both of those cases equations (17) and (18) (or, alternatively, equations (19) and (20)) could be fulfilled for specific combinations of θ_W and θ_S. As one example, the case that equations (17) and (18) both yield $\theta_R = 0$ can be inspected further. By letting the receiver position be expressed as $\theta_R = \epsilon$ (where ϵ is small), the two terms $\nu\varphi_1$ and $\nu\varphi_2$ can be written as

$$\begin{aligned} \nu\varphi_1 &= \frac{\pi}{\theta_W}(\pi + \theta_S + \epsilon) = n_1 \cdot 2\pi + \frac{\pi\epsilon}{\theta_W}, \\ \nu\varphi_2 &= \frac{\pi}{\theta_W}(\pi + \theta_S - \epsilon) = n_1 \cdot 2\pi - \frac{\pi\epsilon}{\theta_W}. \end{aligned}$$

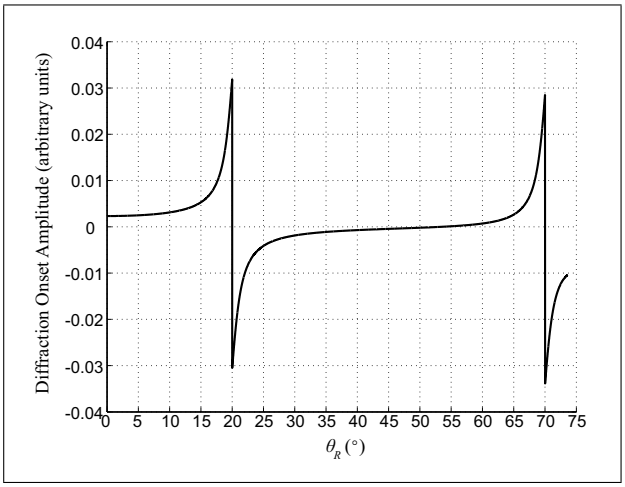

Figure 2. Onset diffraction amplitude as a function of the receiver angle for a 75° wedge and a fixed source at $S = 50°$ (geometry shown in Figure 3). Note the effect of the singularities at 20° ($\nu\varphi_3 = 2\pi$) and 70° ($\nu\varphi_1 = 4\pi$).

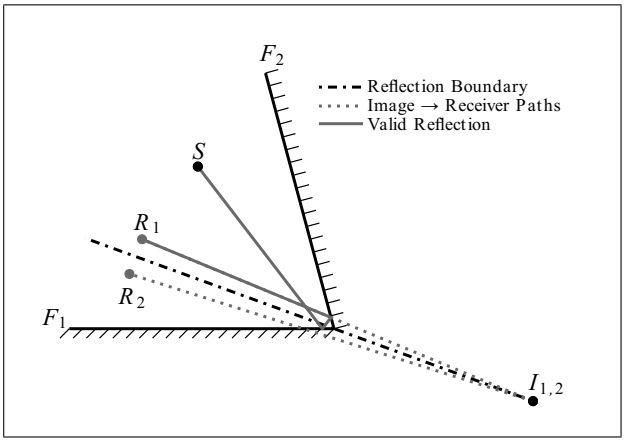

Figure 3. Example geometry: $\theta_W = 75°$, $\theta_S = 50°$, $\theta_{R_1} = 23°$, $\theta_{R_2} = 17°$. The finite extent of the edge (into and out of the page) is not shown for clarity. The boundary shown at $\theta = 20°$ is for the second-order reflection $S \to F_1 \to F_2 \to R$. As shown, a valid reflection exists for receiver R_1 above the boundary, but not for R_2 below the boundary. See also Figure 4.

The opposite signs of the last terms are important since

$$\sin(\nu\varphi_1) = \sin(\frac{\pi\epsilon}{\theta_W}) = -\sin(\nu\varphi_2),$$
$$\cos(\nu\varphi_1) = \cos(\frac{\pi\epsilon}{\theta_W}) = \cos(\nu\varphi_2),$$

which implies that $\beta_1 = -\beta_2$, and those two terms cancel each other in equation (1), also when $\epsilon \to 0$. Similarly, all other (degenerate) cases with singularity-causing receiver positions at $\theta_R = 0$ or $\theta_R = \theta_W$ will generate such cancelling pairs and consequently no singularities will occur.

4. Example Calculations

Consider a wedge with open angle $\theta_W = 75°$ and a source located at $r_S = 8$m, $\theta_S = 50°$, $z_S = 0$m. The behavior of the diffraction onset as a function of a receiver's angular position, θ_R, can be seen in Figure 2, for which a receiver with coordinates $r_R = 8$m and $z_R = 0$m has been swept through all possible angular positions. (The singularity which occurs for the continuous-time impulse response in equation (1) takes on a finite value when discrete-time impulse responses are computed [1]. Thus, the diffraction onset amplitude in Figure 2 is the value of the first non-zero sample of the discrete-time diffraction IR.) The wedge index for this case is $\nu = \pi/\theta_W = 2.4$, and thus equations (15) and (16) predict that singularities can occur only for $\nu\varphi_i = 2\pi, 4\pi$. Two singularities are evident in Figure 2: one at $\theta_R = 20°$ for which $\nu\varphi_3 = 2\pi$, and the other at $\theta_R = 70°$ for which $\nu\varphi_1 = 4\pi$. Per Table I, these are associated with the boundaries for the second-order reflection $S \to F_1 \to F_2 \to R$ and for the third-order reflection $S \to F_2 \to F_1 \to F_2 \to R$, respectively.

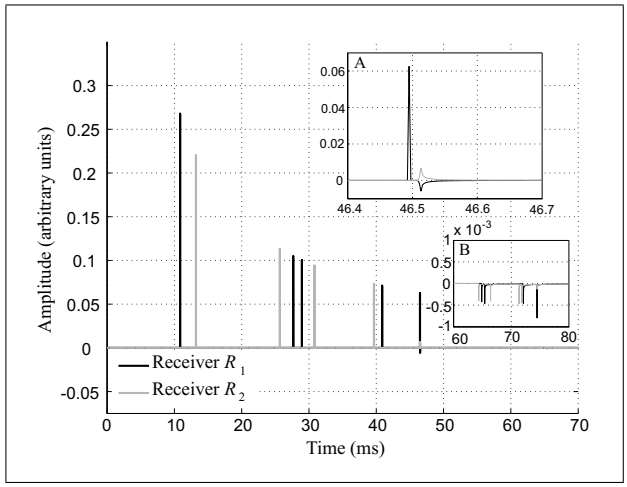

Figure 4. Impulse responses for the example in Figure 3. The main figure shows the full impulse responses. Inset A shows the behavior of the $S \to F_1 \to F_2 \to R$ reflection and the diffracted component. For receiver R_1 the reflection exists and the diffraction polarity is negative. For receiver R_2 there is no reflection and the diffraction polarity has flipped to positive (also seen in Figure 2). Inset B shows the diffracted components from the terminating edges of the wedge faces. Note the zoom extents of the insets.

The example geometry is depicted in Figure 3 along with the behavior near the 20° reflection boundary. For the receiver R_1 with $\theta_R = 23°$ on the "illuminated" side of the boundary, the associated specular reflection is valid and its path is shown. For receiver R_2 with $\theta_R = 17°$ on the "shadowed" side of the boundary, the reflection is not valid. This can be seen by the line segment connecting the image source $I_{1,2}$ with R_2 which does not intersect face F_2 (intersection is a necessary condition for the validity of the reflection). The impulse responses at R_1 and R_2 are depicted in Figure 4. The loss of the reflection for R_2 is evident, as is the change in polarity of the diffraction component at the reflection boundary, also seen in Figure 2. Similar behavior occurs at and near the reflection boundary at 70°. For a receiver with $\theta_R > 70°$, the reflection $S \to F_2 \to F_1 \to F_2 \to R$ exists and the diffraction polarity is negative. For $\theta_R < 70°$ the reflection does not exist and the diffraction polarity is positive.

5. Conclusions

This paper describes the relationship between singularities in first-order diffraction expressions and higher-order reflections related to finite-length wedges for which the open angle is less than π. Such wedges can support second- and higher-order reflections between their faces, and the boundaries for these reflections cause discontinuities in the GA soundfield just as the more

commonly studied shadow boundaries and first-order reflection boundaries do. The diffraction from the edge of the wedge is necessary to maintain a continuous soundfield in the vicinity of the wedge, and the periodicity of the singular behavior, determined by the wedge, source, and receiver geometry, ensures this across all reflection boundaries.

References

[1] U. P. Svensson, P. T. Calamia: Edge-diffraction impulse responses near specular-zone and shadow-zone boundaries. Acta Acustica united with Acustica **92** (2006) 501–512.

[2] W. W. Grannemann, R. B. Watson: Diffraction of electromagnetic waves by a metallic wedge of acute dihedral angle. J. Appl. Phys. **26** (1955) 392–393.

[3] A. V. Osipov: Asymptotic representation of the sound field in a narrow angular region with impedance boundaries. Sov. Phys. Acoust. **36** (1990) 287–290.

[4] M. A. Biot, I. Tolstoy: Formulation of wave propagation in infinite media by normal coordinates with an application to diffraction. J. Acoust. Soc. Am. **29** (1957) 381–391.

[5] A. D. Pierce: Acoustics. McGraw-Hill, New York, 1981.

[6] A. V. Osipov, A. N. Norris: The Malyuzhinets theory for scattering from wedge boundaries: A review. Wave Motion **29** (1999) 313–340.

[7] U. P. Svensson, R. I. Fred, J. Vanderkooy: An analytic secondary source model of edge diffraction impulse responses. J. Acoust. Soc. Am. **106** (1999) 2331–2344.

[8] U. P. Svensson, P. T. Calamia, S. Nakanishi: Frequency-domain edge diffraction for finite and infinite edges. Acta Acustica united with Acustica **95** (2009) 568–572.